

# Experimental and numerical investigation on the performance of an internally cooled dehumidifier

Oguz Emrah Turgut<sup>1</sup> · Mustafa Turhan Çoban<sup>1</sup>

Received: 6 September 2015 / Accepted: 15 February 2016 / Published online: 19 February 2016  
© Springer-Verlag Berlin Heidelberg 2016

**Abstract** Liquid desiccant based dehumidifiers are important components of the air conditioning applications. Internally cooled dehumidifiers with liquid desiccants are deemed to be superior to the adiabatic types, thanks to the cooling medium which takes away the latent heat of vaporization occurred when moist air contacts with liquid desiccant. However, its utilization in industrial applications is restricted due to the inherent corrosive characteristics of the liquid desiccants. In this study, an experimental chamber is built for epoxy coated plate fin type dehumidifier which is used in order to diminish the corrosive effect of the lithium chloride aqueous solution. Dehumidification effectiveness and moisture removal rate, two parameter indices, are adopted to measure the performance of the air conditioning system. The effect of inlet operating parameters on moisture removal rates is extensively analyzed. Two dimensional numerical model adapted from the conservation principles is utilized for obtainment of output parameters. Experimental results are compared with the numerical model and comparisons show that numerical outputs agrees with the experimental results. And also, dehumidification performance of lithium chloride and lithium bromide aqueous solutions are evaluated and compared against each other.

## List of symbols

A Heat and mass transfer area (m<sup>2</sup>)  
Cp Specific heat capacity (kJ/kg K)

H Height of the dehumidifier (m)  
h Enthalpy (kJ/kg)  
h<sub>fg</sub> Latent heat of vaporization (kJ/kg)  
L Length of the dehumidifier (m)  
Le Lewis number (dimensionless)  
 $\dot{m}_{wr}$  Moisture removal rate (g/s)  
 $\dot{m}$  Mass flow rate (kg/s)  
NTU<sub>h</sub> Heat transfer unit number between air and desiccant (dimensionless)  
NTU<sub>m</sub> Mass transfer unit number between air and desiccant (dimensionless)  
P Pressure (kPa)  
T Temperature (°C)  
X Concentration of the liquid desiccant (%)

## Greek symbols

$\alpha$  Heat transfer coefficient between air and desiccant (kW/m<sup>2</sup>K)  
 $\alpha_w$  Heat transfer coefficient between cooling water and desiccant (kW/m<sup>2</sup>K)  
 $\alpha_m$  Mass transfer coefficient between air and desiccant (kg/m<sup>2</sup>s)  
 $\eta$  Dehumidification efficiency (dimensionless)  
 $\omega$  Absolute humidity (kg vapor/kg dry air)

## Subscript

a Air  
da Dry air  
e Air in equilibrium with liquid desiccant  
in Inlet  
out Outlet  
s Liquid desiccant  
v Vapor  
w Cooling water

✉ Oguz Emrah Turgut  
oeturgut@hotmail.com

<sup>1</sup> Mechanical Engineering Department, Ege University,  
35040 Bornova, İzmir, Turkey

## 1 Introduction

Due to the increasing depletion of the conventional energy sources which release high amount of carbon based pollutants out to the atmosphere, global environment pollution is getting worse and worse. High demand on industrialization for better human comfort bring about some unexpected consequences jeopardizing the whole balance of nature that should be given utmost care for better future. Particularly, in the industrialized regions of the world, greenhouse gas emissions nearly reach the health risk limits and with upcoming years it seems to be more threatening due to the economic developments that boost energy consumption rate resulted from the enhanced human activities [1]. According to the reputable sources [2], energy consumption expended by air conditioning facilities from buildings contribute high amount of total energy waste and, with this ongoing trend, it will be very hard to avert this extravagant energy usage. As an alternative to traditional air conditioning systems, liquid desiccant based air conditioning has drawn considerable interest, most particularly for its energy saving nature.

In hot and humid climates, air conditioning is the main challenging issue for occupants not only for maintaining healthy indoor conditions but also improving the quality of labour force. Researchers have made plenty of scientific attempts to overcome this overwhelming subject. One of them is using evaporative cooling in air conditioning systems. Evaporative cooling is famous for its simplicity in operation, low initial and maintenance cost, and consumes lower electrical energy rates compared to other systems [3]. However these systems are quite disadvantageous since they fail to sustain optimal control for all possible climates. Condensing method is another widely used application for absorbing water vapour from moist air. By this method, the air is cooled below its dew point, moisture in the air is condensed and released out to the ambient [4]. In compressing method, the process air is compressed to its saturated pressure at the corresponding temperature and consequently the condense leaves out of the air [5]. Another suitable alternative for air conditioning is absorption or adsorption method. Either liquid or solid, desiccant used in this process absorbs the moisture from air. However, liquid desiccants are superior to solid desiccant types with respect to its inherent advantages such as lower air pressure drop across desiccant material, ease in dust removal by filtration and mobility [6]. Adsorption or absorption performance highly depends on the vapor pressure difference between desiccant and process air. In liquid desiccant air conditioning systems, generally utilize LiCl or LiBr as a liquid desiccant, there are numerous application advantages such as dealing with the latent load [7] and removing number of pollutants including mildew, bacteria etc. [8]. In addition, these systems can procure unlimited humidity control and avoid using high

electrical power that is the main drawback in usage in traditional air conditioning systems [9].

Liquid desiccant systems consist of devices that can control and monitor temperature and humidity separately. These kind of systems can efficiently take advantage of low grade thermal energy such as waste heat and solar energy and successfully manage to handle indoor air quality. Liquid desiccant systems can be nominated as a promising alternative to conventional air conditioning systems with respect to their operational flexibility and sustainable continuity [10]. The use of liquid desiccants in air conditioning processes also maintain effective, economical and environmental—safe cooling and dehumidification [11]. Regenerators and dehumidifiers are the crucial elements of these systems. Dehumidifier is the main component since it sends out water to the concentrated solution in order to facilitate the dehumidification process. Regenerator, in which process air contacts with diluted liquid desiccant, is responsible for regenerating the exhausted desiccant by heating. If it is to attain high success rates on the performance of air conditioning process, substantial care should be given to these components since total system efficiency and effectivity depend on maintaining expected operational conditions.

Specifically, there are two distinctive types of air conditioning system that are dedicated to utilize the liquid desiccants. These are namely internally cooled/heated and adiabatic dehumidifiers. In adiabatic humidifiers, concentrated solution flowing down in the effect of the gravity contact with the humid air. Desiccant solution, which has strong affinity for water vapor, absorbs the moisture available in the process air. However, due to the condensing vapor mixing with the liquid desiccant, heat is released to the system. This emitted heat, composed of latent heat of condensation and chemical energy of mixing liquid desiccant with water vapor, jeopardizes the whole heat and mass transfer process. In order to conquer this drawback, internally cooled dehumidifiers are put into practice in recent years. These type of configurations employ a cooling media to remove the released heat and improve the system efficiency by means of increasing dehumidification capacity. Adiabatic type dehumidifiers are common in industries and more widely used compared to internally cooled dehumidifiers [12, 13]. However, considerable effort has been given to the development of the internally cooled dehumidification systems due to their dense volume [14]. Their inherent complex unit configuration makes these systems less studied than adiabatic ones. Nonetheless, detailed experimental and theoretical studies about internally cooled dehumidification systems have been available for about two decades. Jain et al. [3] experimentally studied the heat and mass transfer characteristics of internally cooled falling film tubular absorber and internally heated falling film plate regenerator.

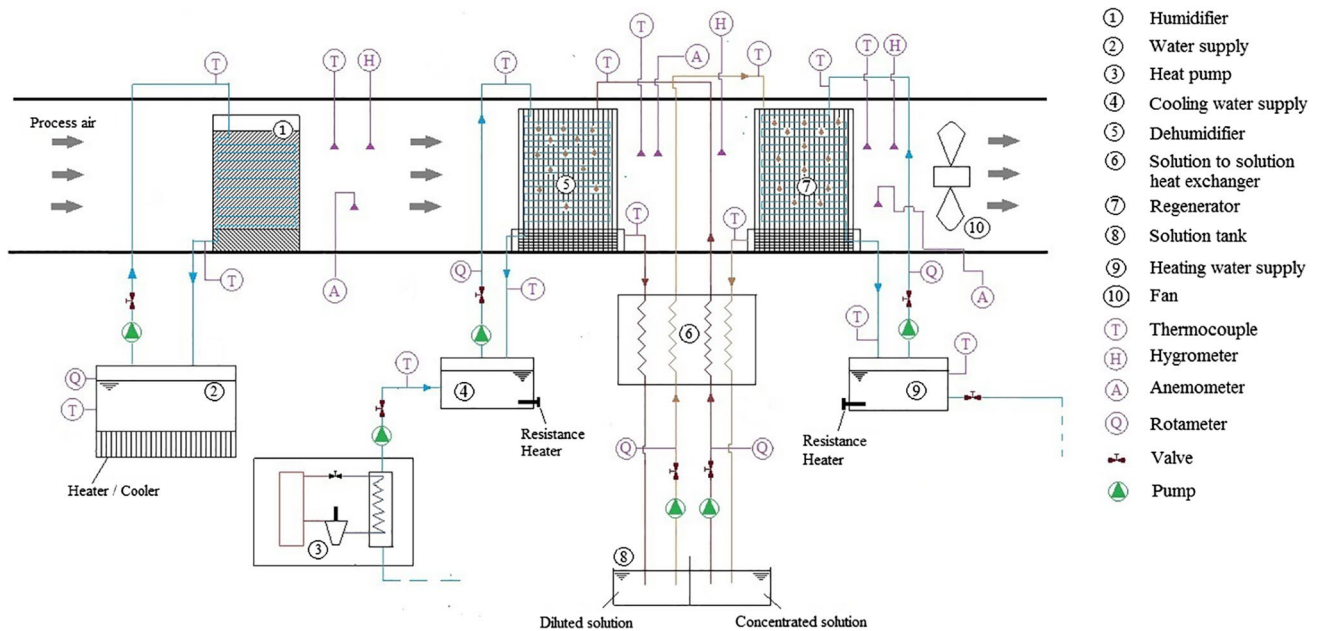


**Fig. 1** Detailed schematic of the experimental setup

To define and explain non-uniform wetting of plate surfaces, two novel wetness factors were introduced. It was revealed that numerical results agree experimental findings with  $\pm 30.0\%$  discrepancy. Saman and Alizadeh [15] proposed a cross flow heat exchanger for both dehumidification and cooling purposes. Results were studied experimentally and numerically. It was found that the heat exchanger gives satisfactory heat and mass transfer performance when liquid desiccant and cooling were used simultaneously. Yin et al. [16] used plate fin heat exchanger for better dehumidification and regeneration performance. In order to investigate varying operating conditions on system efficiency, an experimental setup chamber with a regulable temperature and absolute humidity was utilized. Experimental results showed that cooling efficiency decreases with increasing cooling water and desiccant temperature. Liu et al. [17] numerically investigated the performance of the internally cooled dehumidifier with varying flow direction air to desiccant. Numerical results showed that counter-flow configuration has better dehumidification efficiency whereas parallel flow pattern gives the worst performance owing to the more uniform mass transfer driving force taking part in counter flow configuration. And also, it was mentioned that decrease of the desiccant concentration is the main factor influencing the dehumidification performance. Yin et al. [18] presented a mathematical model for both internally cooled dehumidifier and internally heated regenerator and validated against the experimental results of the internally cooled and adiabatic dehumidifiers. Outcomes of the comparison showed that internally cooled dehumidifier is more

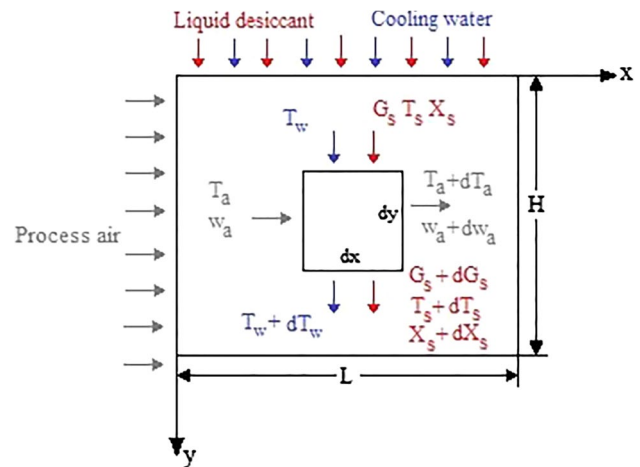


**Fig. 2** 2D model of coupled heat and mass transfer process

efficient than adiabatic dehumidifier in terms of the dehumidification performance. Zhang et al. [14] compared the operating performance of the internally cooled dehumidifier experimentally and numerically. Three novel performance indices namely moisture removal rate, dehumidifying efficiency and volume mass transfer coefficients were adopted to test the effectivity of the dehumidifier made of stainless steel. They found that numerical results agree fairly well with the experimental findings. Luo et al. [19] experimentally and theoretically studied the total performance of the cross flow internally cooled dehumidifier. The proposed dehumidifier, made up fin tube heat exchangers,

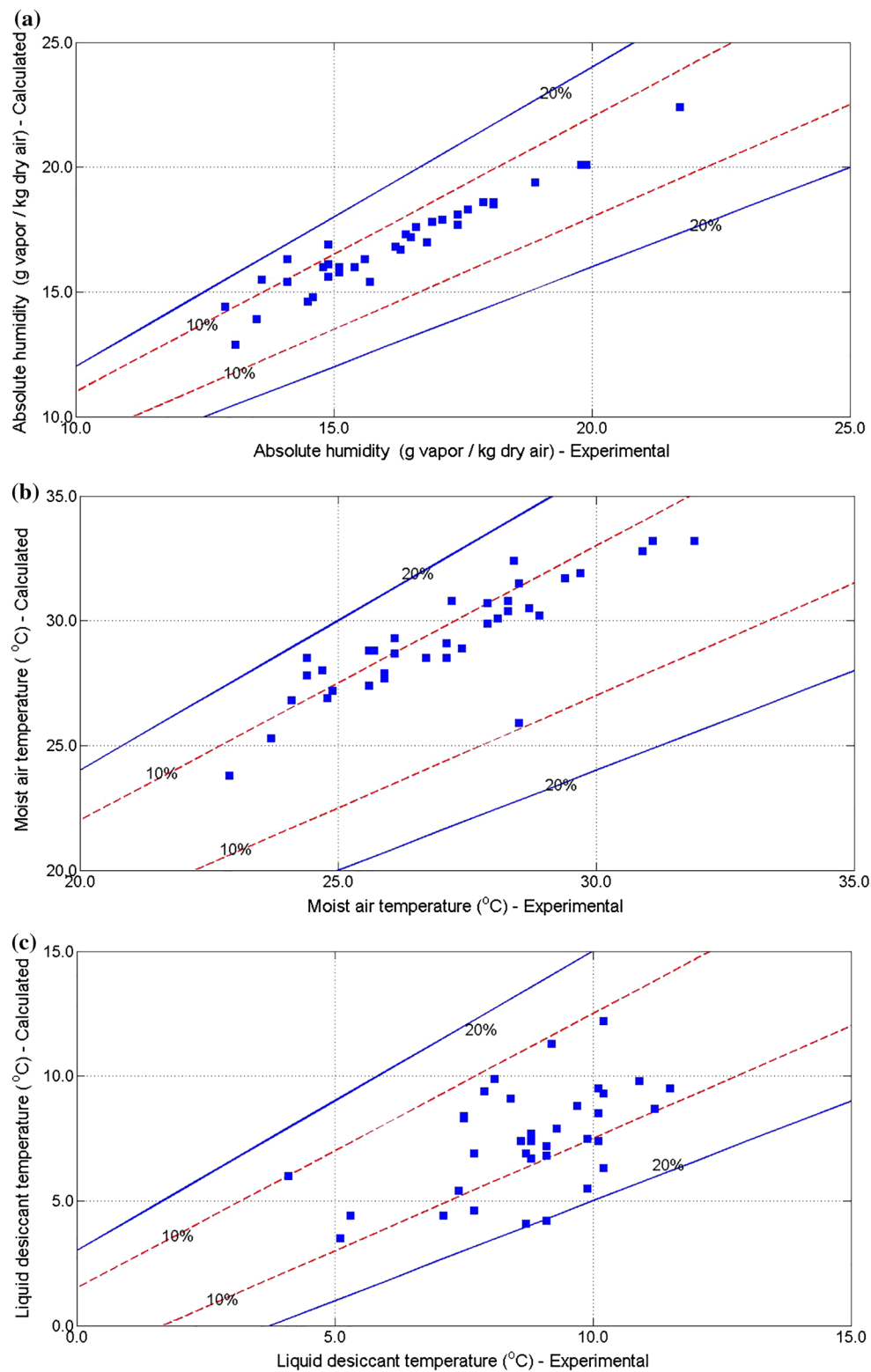


**Fig. 3** **a** Error between experimental and simulated results for absolute humidities. **b** Error between experimental and simulated results for moist air temperatures. **c** Error between experimental and simu-

lated results for liquid desiccant temperatures. **d** Error between experimental and simulated results for cooling water temperatures

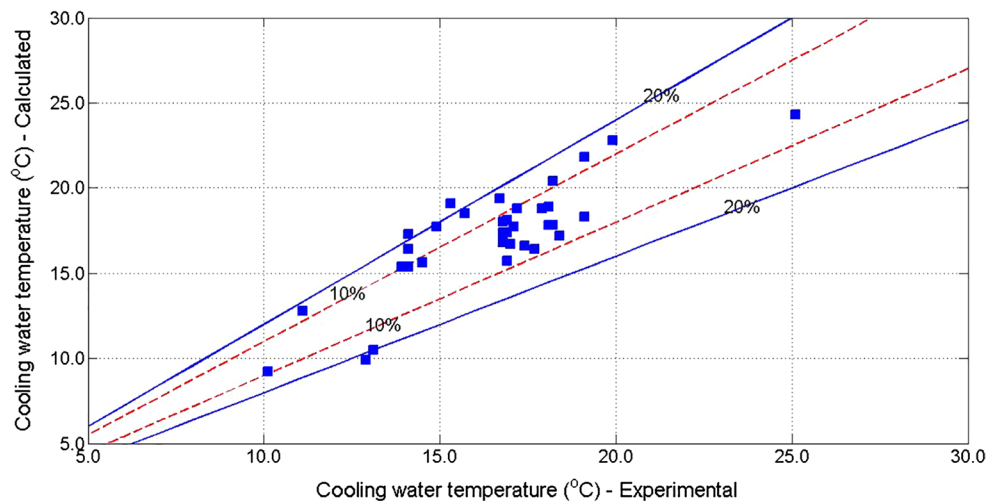


Fig. 3 continued

was assisted with high corrosion resistance. They also correlated heat transfer coefficient based on experimental data which coincides the exact solution with a higher accuracy. Liu et al. [20] presented an internally cooled dehumidifier made of thermally conductive plastic. Propounded plastic coated dehumidifier showed superior corrosive resistance. An experimental setup chamber was used to investigate dehumidification efficiency of dehumidifier with varying operational conditions. The experimental results were compared with that of dehumidifiers made of metal materials available in the literature. Comparisons indicated that proposed dehumidifier gives satisfactory results and has a comparable dehumidification performance concluding that it can be used as a promising alternative for future studies. Luo et al. [2] made experimental and theoretical studies on the dehumidification performance of the single channel internally cooled dehumidifiers. Moisture absorption capacity of the dehumidifier was tested against various conditions. Results showed that application of internally cooled dehumidifier very well suits hot and humid areas where the experiments took place.

All in all, as shown in the literature survey, there are plenty of studies on the performance improvement of internally cooled dehumidifiers. However, it seems that there is still room to upgrade system configuration and improve the total heat and mass transfer efficiency. And also, heat and mass transfer coefficient of the corresponding desiccant moisture absorption system can not be exactly obtained due to the lack of analysis considering the influencing factors on the dehumidification performance. Therefore, in the present study, an experimental set is introduced to attain for better dehumidification process. Experimental rig is operated under different conditions for further and better investigation of influencing parameters. Operating conditions of

the experimental studies are set on the basis of Izmir (Turkey) which is hot and humid in summer climate. In order to diminish the corrosive effect of lithium chloride, an epoxy coated plate fin heat exchangers are used in heat and mass transfer processes. In literature studies, this problem has been thoroughly studied and investigated by researchers. Dehumidifiers made of corrosion resistant metals [21–23] and plastic coated heat exchangers [15, 20] are generally used as a reasonable solution strategy for overcoming the tedious corrosive problem. A numerical model is adopted and validated against the experimental results. It is shown that numerical model is in close agreement with the experimental data.

## 2 Experimental setup

For further investigation of the moisture absorption capability of the internally cooled dehumidifiers, an experimental setting is fabricated in the Energy Laboratory of Ege University, as it is described in Fig. 1. Total size of the test channel is  $600 \times 700 \times 2000$  mm. Test section is composed of three distinct conditioning units. These are pre-conditioned air unit, dehumidification and regeneration sections. Part 1, consisting of filler made of detailed paper, is responsible for controlling the absolute humidity and inlet air temperature. In order to change air speed, test rig is equipped with a frequency conversion speed regulation unit. Part 2 has a desiccant control unit and cooling water storage tanks. This section deals with the absorption of moisture from the process air with an epoxy coated dehumidifier. Dehumidifier has copper tubes having 15.4 mm inner diameter and 17.2 outer diameter. Distance between two consecutive fins is 2.5 mm. Water storage tank, made

of 2.0 mm thick galvanized steel sheet having dimensions of  $500 \times 500 \times 500$  mm, stores the cooling water which is circulated through the pumps. A resistance heater welded to the storage tank regulates the circulated water drained from the heat pump. Part 3 has a regenerator unit which has the same characteristics of the dehumidifier taking place in Part 2 and hot water storage tank having identical physical properties of cold water tank. Hot water tank is filled with tap water and water temperature in the tank is controlled by resistance heater as done in the cold water tank. Liquid desiccant, hot and cold water mass flow rates are adjusted by the ball valves.

Process air, propelled by the fan at the exit of the test channel, enters the test section and conditioned in the pre-conditioned air unit which is made of honeycomb filler. After this section, conditioned air enters the epoxy coated dehumidifier and releases out the excess moisture.

**Table 1** Range of the operational parameters

| Parameter                       | Symbol          | Unit                              | Range         |
|---------------------------------|-----------------|-----------------------------------|---------------|
| Air flow rate                   | $m_a$           | kg/s                              | 0.17–0.74     |
| Inlet air humidity              | $\omega_{a,in}$ | kg <sub>v</sub> /kg <sub>da</sub> | 0.0214–0.0158 |
| Inlet air temperature           | $T_{a,in}$      | °C                                | 24.1–32.6     |
| Inlet solution temperature      | $T_{s,in}$      | °C                                | 19.7–29.6     |
| Solution flow rate              | $m_s$           | kg/s                              | 0.22–0.67     |
| Inlet cooling water temperature | $T_{w,in}$      | °C                                | 5.4–18.1      |
| Cooling water flow rate         | $m_w$           | kg/s                              | 0.21–0.72     |

In internally cooled dehumidification tests, water available in the storage tanks are used as a cooling media to improve the moisture absorption capability. Simultaneously, concentrated liquid desiccant solution (lithium chloride) pumped through the Pprc pipes and sprinkled over the plate fin heat and mass exchanger forming tiny particles reassuring that liquid desiccant droplets spread uniformly on the exchanger surface. Diluted liquid desiccant arrives the desiccant tank and is sent to the regenerator to be re-concentrated. At this time, process air flow past the dehumidifier and reaches up the regenerator. Hot water obtained from the storage tank heats the diluted liquid desiccant and increases its vapor pressure. Consequently, desiccant solution gives off the water vapor, becomes concentrated and is sent to the strong solution tank to be used as a moisture absorber in the dehumidifier.

Experiments were conducted within predefined ranges in order to reflect the effect of influence of varying operational conditions. Initial parameters of air mass flow rate was adjusted by simple electric voltage regulator. Air humidity and temperature were adjusted by Nuve Bd—402 water bath, having the ability of both monitoring and controlling of these parameters. Inlet temperatures of desiccant solution and cooling water were measured by Pt RTD thermocouples and recorded by the Testo 454 control unit. Maximum error between recorded and exact temperature is 0.3 K. Maximum air humidity is in the range between 0.2 and 0.4 g/kg

**Table 2** Some of test results for dehumidification process

| $T_{a,in}$ (°C) | $T_{a,out}$ (°C) | $\omega_{a,in}$ (g/kg) | $\omega_{a,out}$ (g/kg) | $T_{s,in}$ (°C) | $T_{s,out}$ (°C) | $T_{w,in}$ (°C) | $T_{w,out}$ (°C) | $m_s$ (kg/s) | $m_w$ (kg/s) | $m_a$ (kg/s) |
|-----------------|------------------|------------------------|-------------------------|-----------------|------------------|-----------------|------------------|--------------|--------------|--------------|
| 26.6            | 23.7             | 16.7                   | 13.5                    | 21.1            | 19.1             | 14.3            | 16.9             | 0.28         | 0.28         | 0.35         |
| 25.4            | 22.9             | 16.1                   | 13.1                    | 24.3            | 20.3             | 12.1            | 15.7             | 0.24         | 0.24         | 0.33         |
| 28.7            | 25.6             | 17.1                   | 14.5                    | 28.1            | 25.2             | 14.1            | 18.2             | 0.34         | 0.41         | 0.35         |
| 29.7            | 25.7             | 17.4                   | 15.7                    | 29.4            | 26.2             | 17.9            | 19.9             | 0.36         | 0.38         | 0.44         |
| 31.7            | 29.4             | 19.6                   | 17.1                    | 28.3            | 26.5             | 14.6            | 17.1             | 0.46         | 0.46         | 0.32         |
| 32.8            | 29.7             | 21.4                   | 18.9                    | 27.7            | 24.2             | 13.7            | 16.8             | 0.43         | 0.41         | 0.33         |
| 29.8            | 27.4             | 19.4                   | 16.5                    | 28.1            | 25.1             | 16.1            | 19.1             | 0.12         | 0.41         | 0.34         |
| 31.2            | 28.1             | 21.4                   | 18.1                    | 26.1            | 25.2             | 13.7            | 17.9             | 0.14         | 0.28         | 0.80         |
| 29.9            | 27.1             | 19.8                   | 16.9                    | 25.9            | 22.5             | 13.9            | 18.2             | 0.30         | 0.50         | 0.30         |
| 31.2            | 27.9             | 20.0                   | 16.6                    | 26.1            | 23.8             | 14.2            | 17.7             | 0.21         | 0.54         | 0.36         |
| 30.2            | 26.1             | 18.7                   | 14.9                    | 28.3            | 25.9             | 20.1            | 24.3             | 0.27         | 0.32         | 0.38         |
| 35.0            | 31.9             | 23.1                   | 19.8                    | 26.2            | 23.8             | 10.9            | 14.1             | 0.26         | 0.31         | 0.46         |
| 31.7            | 27.9             | 19.1                   | 16.4                    | 27.3            | 24.1             | 13.2            | 16.8             | 0.27         | 0.28         | 0.21         |
| 30.7            | 24.1             | 18.5                   | 12.9                    | 28.1            | 20.1             | 5.6             | 14.1             | 0.25         | 0.31         | 0.35         |
| 30.4            | 27.5             | 19.1                   | 14.9                    | 28.1            | 23.7             | 6.1             | 13.1             | 0.31         | 0.37         | 0.39         |
| 30.0            | 28.5             | 18.7                   | 14.8                    | 28.6            | 24.1             | 5.4             | 10.1             | 0.27         | 0.50         | 0.32         |



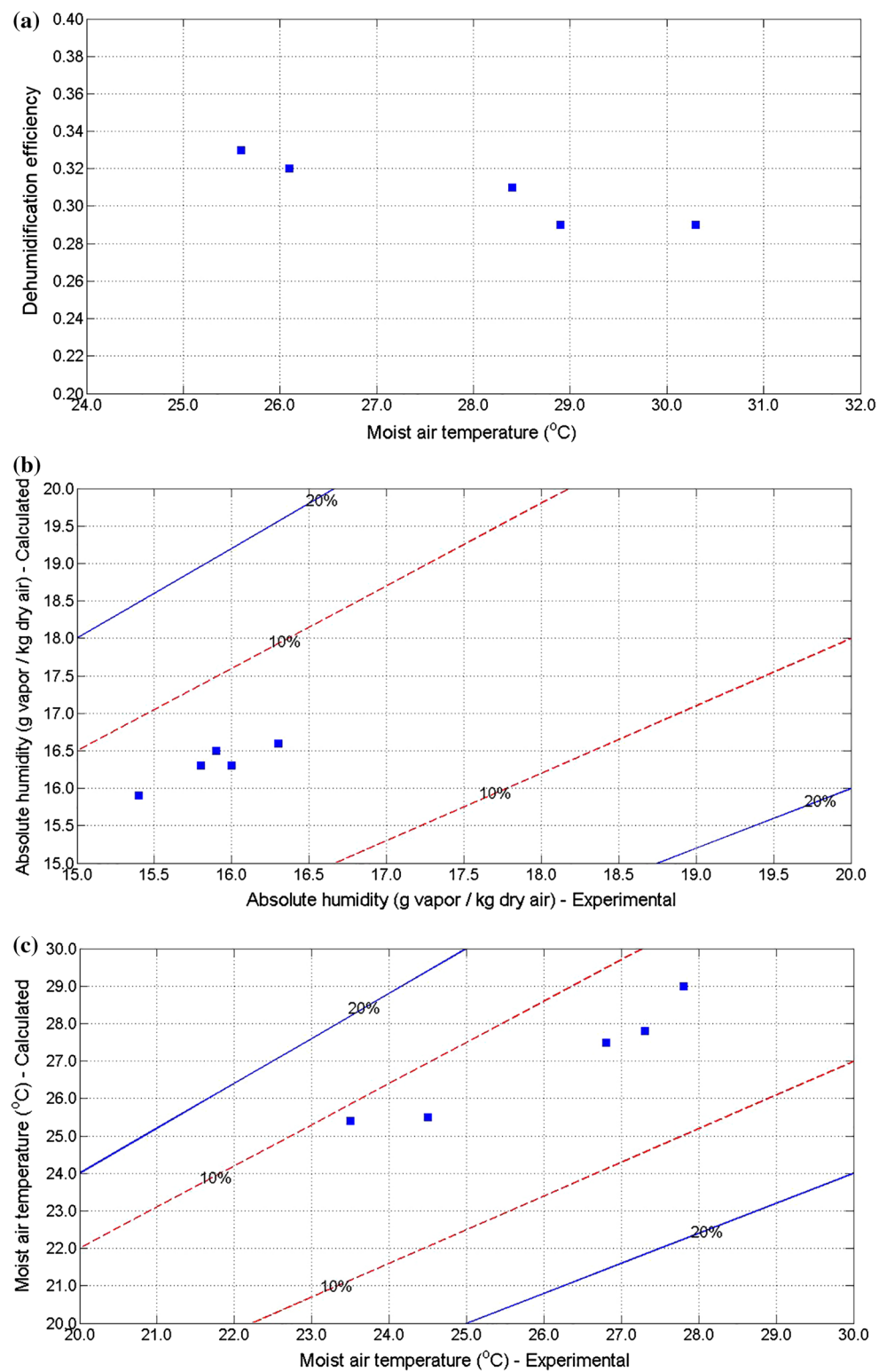


**Fig. 4** **a** Dehumidification efficiencies according to changing moist air temperatures. **b** Error band representation for outlet absolute humidities for varying inlet moist air temperatures. **c** Error band representation for outlet air temperatures for varying inlet moist air temperatures

### 3 Mathematical modelling of heat and mass transfer for internally cooled dehumidifier

In order to validate and evaluate the experimental results, heat and mass transfer model is developed. Figure 2 shows the coupled heat and mass transfer process of internally cooled dehumidifier. Air flowing through the dehumidifier is perpendicular to the cooling water flowing through the pipes and the falling film liquid desiccant film on the fin surface. For modelling the heat and mass transfer phenomena, following assumptions are made [24, 25]

- Heat and mass transfer with the environment is neglected
- Steady state heat transfer is considered
- Thermophysical properties within the infinitesimal control volume is assumed to be constant

- Heat and mass transfer areas are assumed to be same
- No chemical reaction is considered between moist air and liquid desiccant

Taking into consideration of the above mentioned assumptions, basic energy and mass conservation equations of the heat and mass transfer processes in the internally cooled dehumidifier can be defined as follows:

$$\frac{\dot{m}_a}{H} \frac{\partial h_a}{\partial x} + \frac{1}{L} \frac{\partial (\dot{m}_s h_s)}{\partial y} + C_{p,w} \frac{\dot{m}_w}{L} \frac{\partial T_w}{\partial x} = 0 \quad (1)$$

$$\frac{\dot{m}_a}{H} \frac{\partial \omega_a}{\partial x} + \frac{1}{L} \frac{\partial \dot{m}_s}{\partial y} = 0 \quad (2)$$

$$\frac{\partial (\dot{m}_s X)}{\partial y} = 0 \quad (3)$$

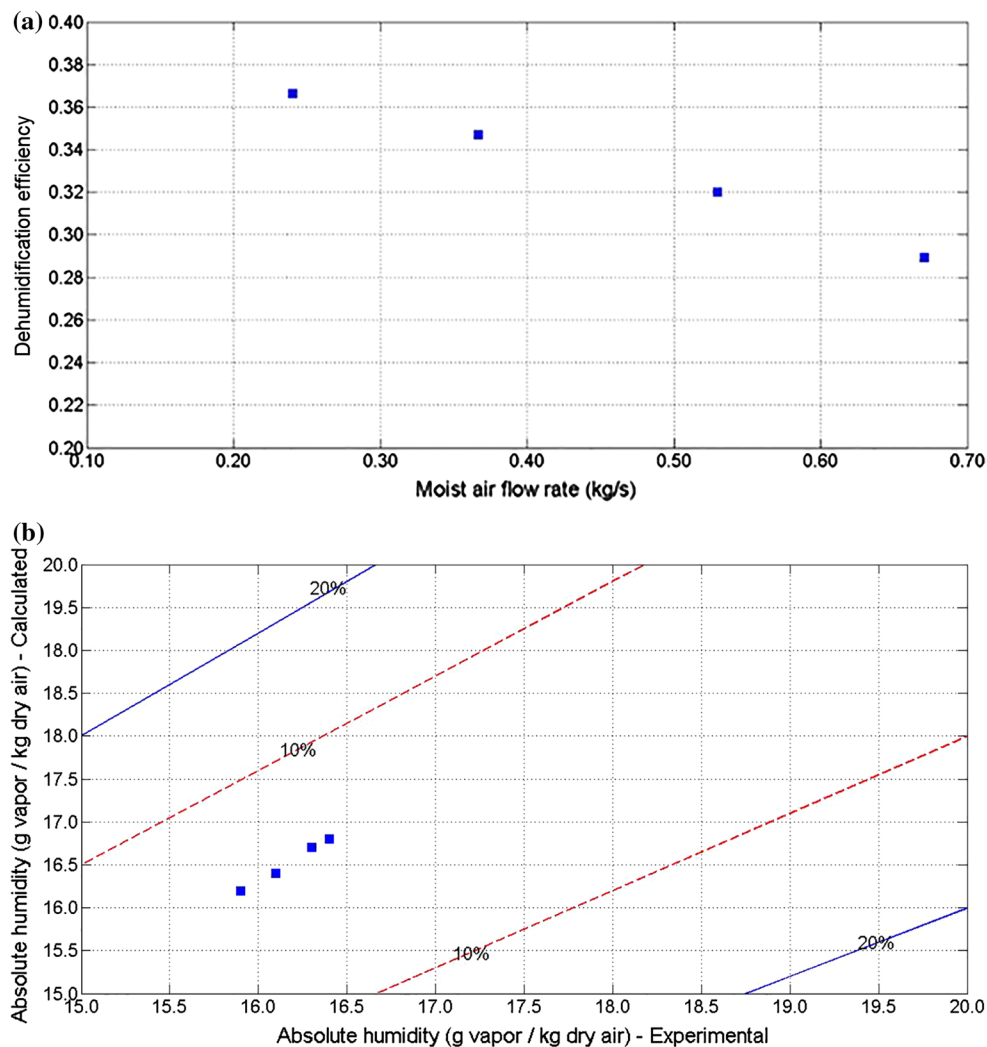


**Fig. 5** **a** Dehumidification efficiencies for changing air flow rates. **b** Discrepancies between experimental and calculated results for absolute humidities



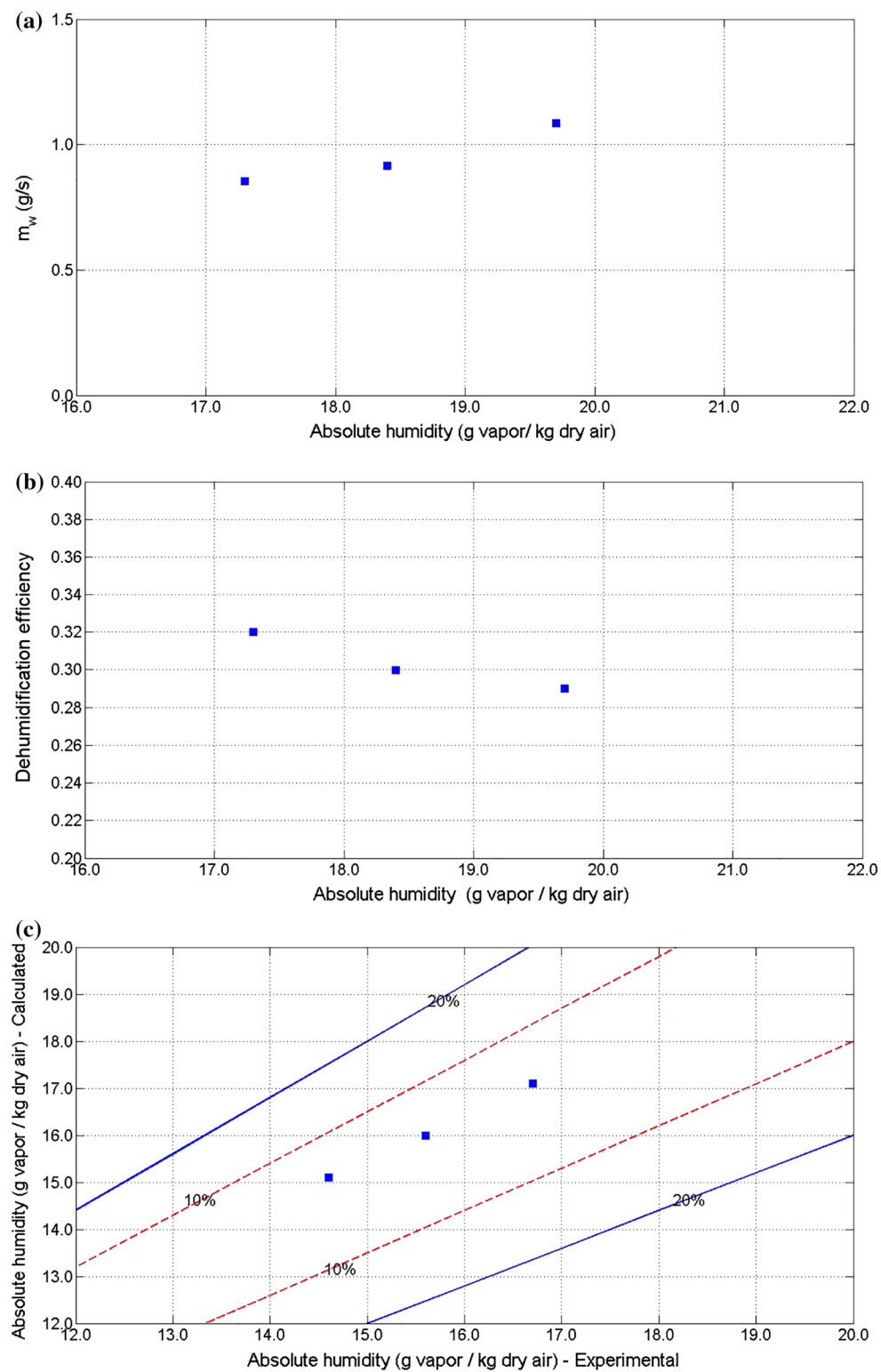


**Fig. 6** **a** Effect of humidity ratios on the moisture removal rates. **b** Effect of humidity ratios on the dehumidification efficiencies. **c** Variation between simulated and experimental results for outlet absolute humidities for changing inlet humidity ratios

Energy transfer between cooling water and the liquid desiccant can be modeled by Eq. (4):

$$\frac{\partial T_w}{\partial y} = \frac{NTU_h}{L}(T_w - T_s) \quad (4)$$

Heat and mass transfer between the process air and the liquid desiccant can be expressed by Eqs. (5) and (6):

$$\frac{\partial h_a}{\partial x} = \frac{NTU_m \cdot Le}{L} \left[ (h_e - h_a) + h_{fg} \left( \frac{1}{Le} - 1 \right) (\omega_e - \omega_a) \right] \quad (5)$$

$$\frac{\partial \omega_a}{\partial x} = \frac{NTU_m}{L} (\omega_e - \omega_a) \quad (6)$$

$$NTU_h = \frac{\alpha_w A}{C_{p,w} \dot{m}_w}, \quad NTU_m = \frac{\alpha_m A}{\dot{m}_a}, \quad Le = \frac{\alpha}{\alpha_m C_{p,a}} \quad (7)$$

Initial conditions of air, desiccant solution and cooling water are expressed by the following equations.

$$x = 0, \quad T_a = T_{a,in}, \quad \dot{m}_a = \dot{m}_{a,in}, \quad \omega_a = \omega_{a,in} \quad (8)$$

$$y = 0, \quad T_s = T_{s,in}, \quad \dot{m}_s = \dot{m}_{s,in}, \quad X_s = X_{s,in} \quad (9)$$

Considering these equations, coupled heat and mass transfer model is built to predicate outlet conditions of operating parameters. Figure 3a–d gives the comparison between calculated and experimental values for outlet conditions of absolute humidity, moist air temperature, cooling water temperature and liquid desiccant temperature. From the figures, it can be concluded that the proposed model can be conveniently applied to the modelling of dehumidification process according to the negligible discrepancies between simulated and experimental results which is kept within  $\pm 20\%$  error band.

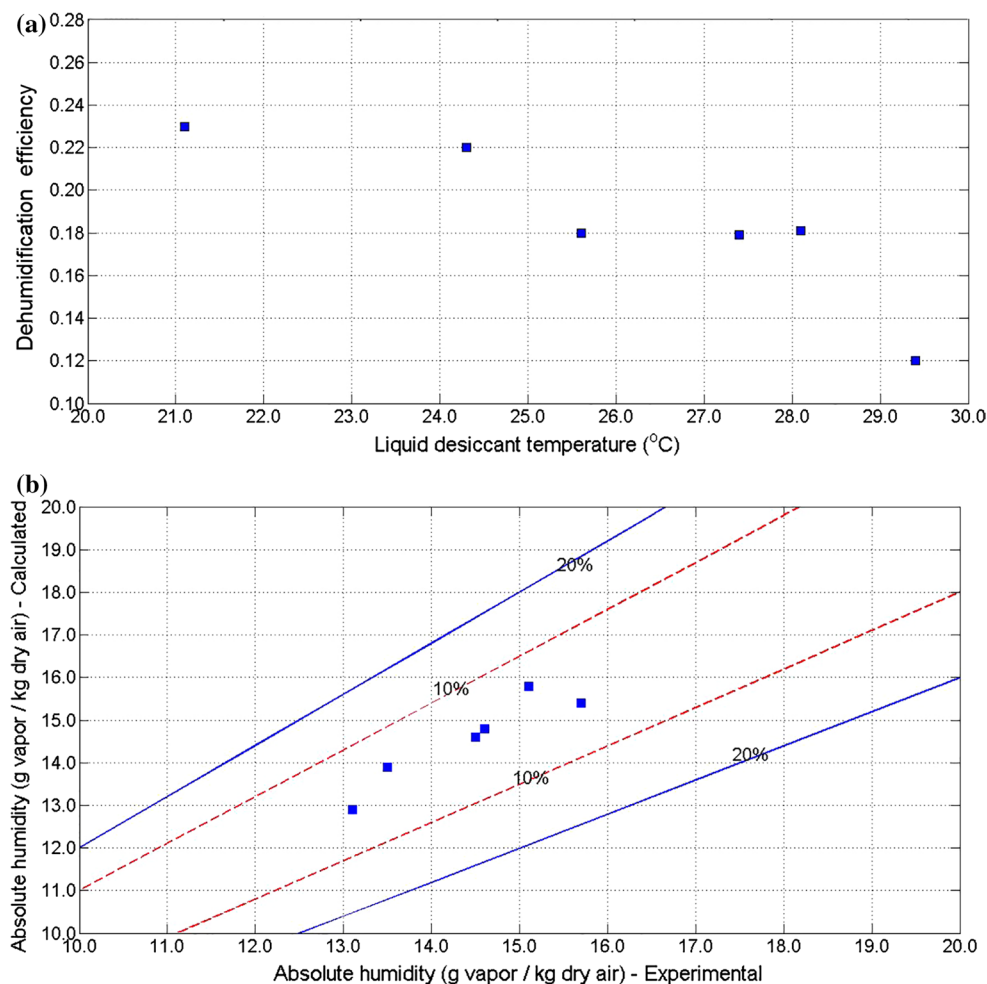


**Fig. 7** **a** Effect of liquid desiccant temperatures on the absorber efficiencies. **b** Error between calculated and experimental results for absolute humidities

#### 4 Experimental results and influencing factors

Lithium chloride aqueous solution (LiCl) is used in the experiments as a moisture absorber/desorber. Influencing factors of air temperature, absolute humidity, cooling water flow rate, cooling water temperature, liquid desiccant flow rate, liquid desiccant temperature on system performance have been discussed for further understanding of the effect of operational conditions. Table 1 gives the limits of the operational conditions for influencing parameters reported in Table 2 and shown in Figs. 3, 4, 5, 6, 7, 8, 9, and 10. Table 2 shows some of the stable experimental results obtained from tests.

Some performance indices have been introduced to validate the dehumidification process for all possible conditions. Mass transfer performance of the system is assessed in terms of dehumidification flow rate (g/s) by the following equation

$$\dot{m}_{wr} = \dot{m}_a(\omega_{in} - \omega_{out}) \quad (10)$$

Dehumidification efficiency ( $\eta$ ) is used to measure absorption capacity of the dehumidifier under predefined working conditions and can be represented as

$$\eta = \frac{\omega_{in} - \omega_{out}}{\omega_{in} - \omega_e} \quad (11)$$

where  $\omega_e$  stands for the water content of air in equilibrium with the surface temperature of the liquid desiccant solution. These indices are utilized for assessing the performance of the mentioned dehumidification test rig and finding out the influencing effect of the operational parameters. Figure 4a shows the effect of inlet air temperatures on the dehumidification efficiencies. It is seen that increasing air temperatures reduce the dehumidification efficiencies. The same behaviour is also encountered

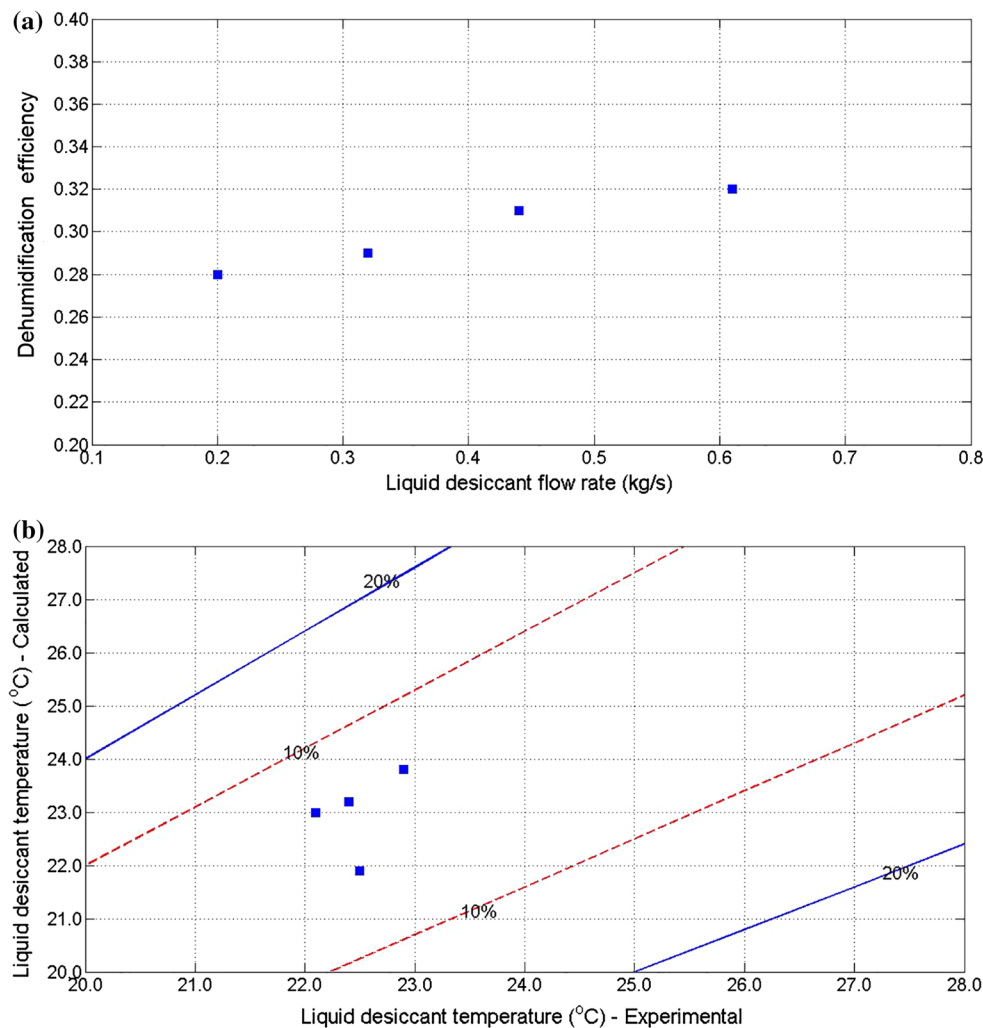


**Fig. 8** **a** Influence of liquid desiccant flow rate on dehumidification efficiencies. **b** Discrepancies between calculated and experimental results for liquid desiccant solution temperature for varying solution mass flow rates

in [2, 19, 26]. Liquid desiccant having lower water partial pressure suffers from limited water evaporation which eases the mass transfer from the ambient. Sensible heat transfer from the moist air increases surface temperature of the liquid desiccant raising the water partial vapor pressure in the desiccant solution. This will consequently reduces the mass transfer capability of the process resulting in lower dehumidification efficiencies. Figure 4b, c compares the experimental results against simulated values for outlet absolute humidities and air temperatures for varying inlet air temperatures. Figure 5a shows the effect of air flow rate on the dehumidification efficiency of the absorber at particular experimental conditions. Test results for this case show that dehumidification efficiencies deteriorate with increasing air mass fluxes. This is because of high air velocities lead to reduced residence time in the absorber and result in limited mass transfer rates between

moist air and liquid desiccant solution. [2, 27]. Figure 5b gives the comparison between simulated and experimental results. Negligible errors are seen between two terms. Figure 6a shows the condensation rate in the dehumidifier with varying absolute humidities. Considering the figure, it can be concluded that increasing absolute humidities enhances moisture removal ability in the absorber. This tendency is reasonable for this case since inherent water content in the moist air increases with increasing humidity ratio values. This will decrease equilibrium humidity ratio, enhance the average water vapor difference and gives considerable potential for mass transfer. Figure 6b shows the effect of humidity ratio on the absorption performance of the dehumidifier. As seen from the figure, increasing absolute humidities degrades the dehumidification efficiency of the absorber. This behavior can be attributed to the variational change in the ratio between

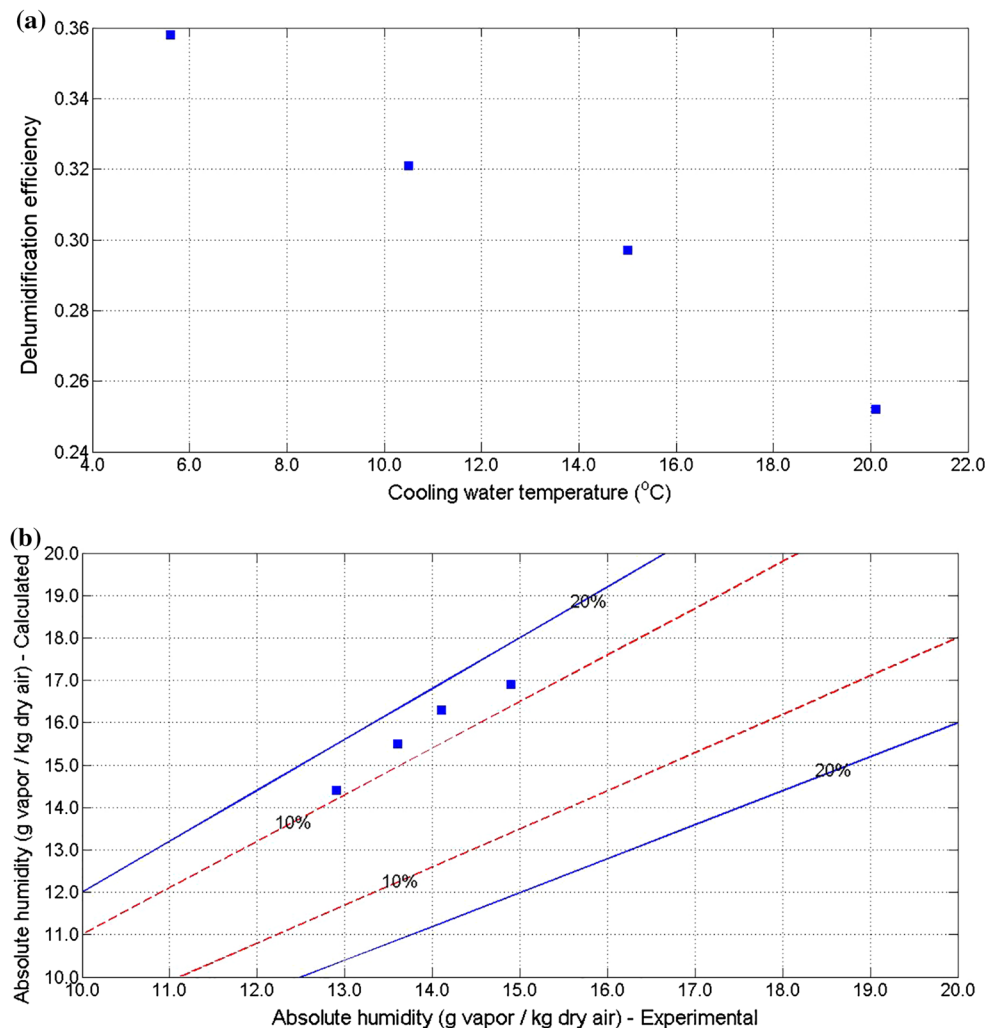


**Fig. 9** **a** Effect of cooling water temperatures on dehumidification efficiencies. **b** Error between calculated and experimental results for absolute humidities for varying cooling water temperatures

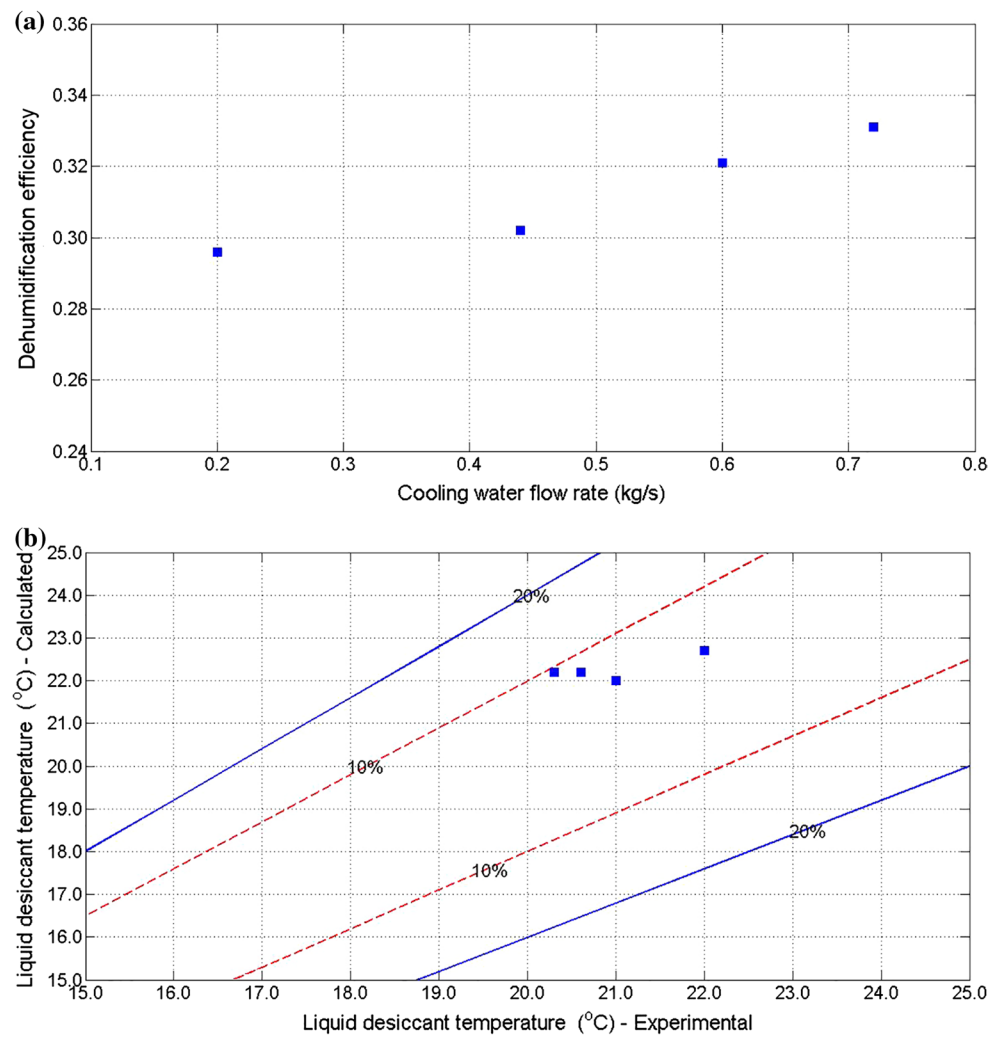


**Fig. 10** **a** Effect of cooling water flow rates on dehumidification efficiencies. **b** Experimental versus simulated results for solution temperatures for varying cooling water mass flow rates

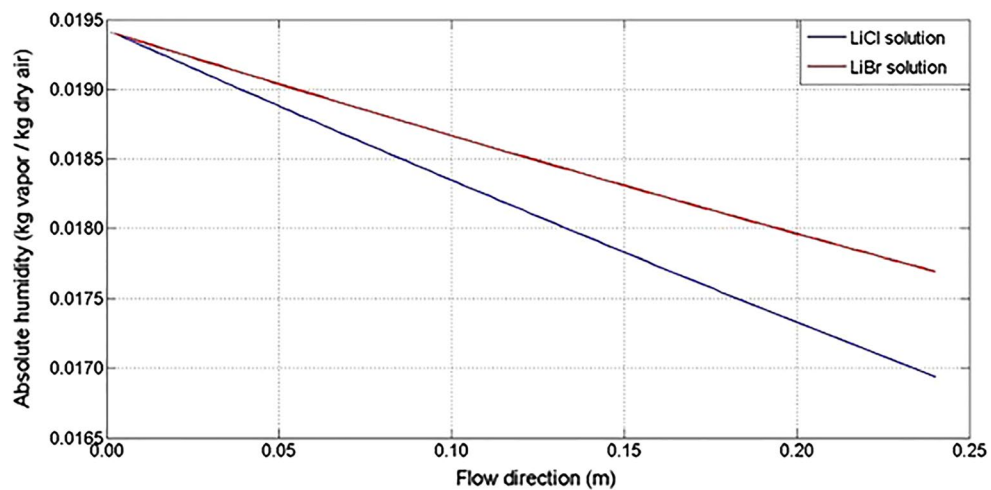


**Fig. 11** Humidity ratio variation of the process air with different working solutions

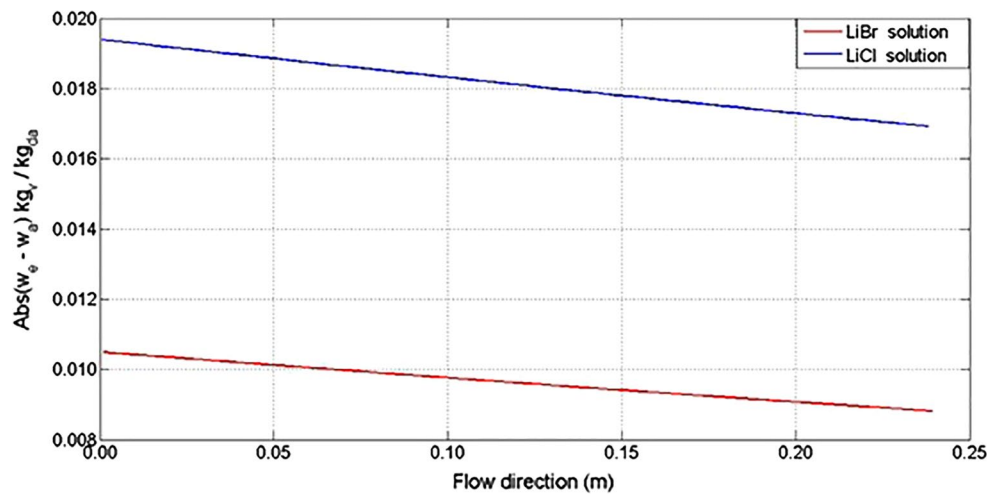
**Table 3** Thermophysical properties of LiCl and LiBr solutions

| $T_s$ (°C) | X (%) | LiCl solution                                  |                 | LiBr solution                                  |                 |
|------------|-------|--|-----------------|--|-----------------|
|            |       | $\omega_e$ (g <sub>v</sub> /kg <sub>da</sub> ) | $P_{sat}$ (kPa) | $\omega_e$ (g <sub>v</sub> /kg <sub>da</sub> ) | $P_{sat}$ (kPa) |
| 20.0       | 30.0  | 6.046  | 0.975           | 10.672   | 1.709           |
| 20.0       | 31.0  | 5.638  | 0.910           | 10.441   | 1.672           |
| 20.0       | 32.0  | 5.239  | 0.846           | 10.197   | 1.634           |
| 20.0       | 33.0  | 4.853  | 0.784           | 9.940  | 1.593           |
| 20.0       | 34.0  | 4.481  | 0.724           | 9.670  | 1.551           |
| 20.0       | 35.0  | 4.125  | 0.667           | 9.385  | 1.506           |
| 20.0       | 36.0  | 3.787  | 0.613           | 9.084  | 1.458           |
| 20.0       | 37.0  | 3.467  | 0.561           | 8.768  | 1.408           |
| 20.0       | 38.0  | 2.885  | 0.513           | 8.437  | 1.356           |
| 20.0       | 39.0  | 2.624  | 0.467           | 8.090  | 1.301           |
| 20.0       | 40.0  | 2.381  | 0.425           | 7.728  | 1.243           |

nominator ( $\omega_{in} - \omega_{out}$ ) and denominator ( $\omega_{in} - \omega_e$ ) in Eq. (11). Figure 6c depicts the deviation between experimental and calculated results for outlet humidity ratios for varying inlet absolute humidities. It can be concluded that numerical results fairly agrees with the experimental findings for this case. Figure 7a shows the influence of liquid desiccant solution temperature on system efficiencies. As it is shown in figure, absorber efficiencies decrease with increasing solution temperatures. In particular experimental conditions, temperature increase in the whole system causes exponential increase in water vapor pressure which decrease water vapor pressure difference between working fluids inducing considerable drop in potential moisture mass transfer capacity from air to desiccant solution. Furthermore, as it was stated in [2], interaction between moist air and liquid desiccant solution leads to significant rise in latent heat of absorption which fully jeopardize the dehumidification process. This deterioration can be either solved by introducing a cooling media to the absorption system or decreasing working solution temperatures. Figure 7b shows the calculated and test results for absolute humidity rates. It is observed that error between two terms are kept within  $\pm 10\%$  for all test cases. Figure 8a shows the effect of liquid desiccant solution mass flow rate on the moisture absorption efficiency. Increasing mass flow rate of solution leads to maintain higher heat capacity of the solution which allows small temperature gradients along the dehumidifier length procuring lower temperature rise on the solution surface. Also, higher mass velocities give rise to increase total wetting area between desiccant solution and moist air. However, in our experiments, there is only slight increase in dehumidification efficiency rates. Same observation was also encountered in [2]. Figure 8b depicts the error between calculated and test results for liquid desiccant solution temperatures for varying solution

flow rates. As seen, experimental results clearly agrees with the numerical solutions. Figure 9a compares the effect of cooling water temperatures on the absorber performance. It is seen that moisture absorption performance is greatly reduced by increasing cooling water temperatures. Low temperature water flowing through the tubes engenders heat transfer from liquid desiccant solution to ambient. This process not only decreases the surface temperature of solution causing a drop in water vapor pressure but also reduce the effect the temperature rise occurred by the latent heat of absorption and thereby, water vapor difference between liquid desiccant and moist air increases which promotes mass transfer rates. Figure 9b delineates the difference between simulated and experimental results for absolute humidities for changing water cooling temperatures. For this case, experimental data is slightly overpredicted by the numerical model as it is observed that numerical findings go beyond  $\pm 10\%$  error zone. Figure 10a compares the cooling water flow rate effect on the absorption performance of the dehumidifier. It is found that increase in cooling water flow rates leads to a slight elevation in dehumidification efficiency values. As mass flow rate of cooling water increases, its heat capacity and corresponding Reynolds number increases as well. This increase causes a certain rise in heat transfer rates between cooling water and desiccant solution conducting a lower surface vapor pressure as a result of decreased solution temperatures. Therefore, driving force of the mass transfer increases, causing higher effective absorption mechanism compared to low cooling water mass flow rate design. However, Luo et al. [2] reported that cooling media flow rate variation does not effect on the performance of the dehumidifier while the same influence did not take part in the work of Liu et al. [20]. Figure 10b shows the deviation between simulated and test results for outlet desiccant solution temperatures under the effect of varying cooling water flow rates. Figure 11 compares the absorption performance of the LiCl and LiBr solutions along the flow direction under the same experimental conditions. As seen, dehumidification performance of the absorber with LiCl solution is better than that of the absorber with LiBr solution. Thermodynamic properties of the solutions take a great role in shaping the absorption performance of the dehumidifier. Table 3 reports the equilibrium humidity ratios and water vapor pressures of LiCl and LiBr solutions with varying solution concentrations under the same solution temperature. It is observed that vapor pressures of the LiCl solution is lower than that of that LiBr solution for each comparison case. Desiccant vapor pressure rate is the key factor that determines the dehumidification effectivity in the course of mass transfer process. Equilibrium humidity ratio decreases with lower desiccant vapor pressures.



**Fig. 12** Difference between equilibrium humidity ratio of the desiccant and actual absolute humidity of air along with flow direction

This reduction increases the gap in the right side of Eq. (6) and promotes the driving force for the mass transfer.

Figure 12 compares the difference between desiccant equilibrium humidity and humidity ratio of the process air along the flow direction for LiCl and LiBr solutions. Dehumidifier working with LiCl solution has more options for mass transfer due to the aforementioned vapor pressure effect. It is also seen that difference between two terms has tendency to decrease along the flow channel as a result of decreasing water removal rate from the solution.

## 5 Conclusion

In this study, cross flow plate fin dehumidifier is experimentally and numerically investigated. Surface of the plates are coated with epoxy in order to minimize the jeopardizing effect of the corrosion. The effect of operating parameters on the dehumidification performance is detailly analyzed. From the experimental results, following conclusions can be drawn:

1. Internally cooled dehumidifier coated with epoxy was designed and it was observed that plates coated with epoxy can withstand the corrosive effect of aqueous lithium chloride solution. However, as time passed by, water removal efficiency of the dehumidifier was reduced due to the harmful effect of the corrosion.
2. Results obtained from the two dimensional mathematical model agreed with the experimental results. Based on this agreement, dehumidification performance of

the aqueous solutions of lithium chloride and lithium bromide were compared. It was found that lithium chloride solution attains better dehumidification rates.

3. Cooling water and desiccant temperatures greatly influence the water absorption capability of the dehumidifier. Lower values of these operating parameters enhance the moist absorption from the process air due to the drastic increase in water vapor pressures
4. Cooling water and solution mass flow rates slightly affect the water removal rate of the dehumidifier.
5. Corrosion problem should be taken more seriously for better and efficient dehumidifier design.

## References

1. Enteria N, Mizutani K (2011) The role of the thermally activated desiccant cooling technologies in the issue of energy and environment. *Renew Sust Energy Rev* 15:2095–2122
2. Luo Y, Wang M, Yang H, Lu L, Peng J (2015) Experimental study of internally cooled liquid desiccant dehumidification: application in Hong Kong and intensive analysis of influencing factors. *Build Environ* 93:210–220
3. Jain S, Dhar P, Kaushik SC (2000) Experimental studies on the dehumidifier and regenerator of a liquid desiccant cooling system. *Appl Therm Eng* 20:253–267
4. Li Z, Liu XH, Lun Z, Jiang Y (2010) Analysis on the ideal energy efficiency of dehumidification process from buildings. *Energy Build* 42:2014–2020
5. Ouyang YX, Wang JF, Liu JQ (2000) Research on the cycle of dehumidifying by compressing the air. *J Fluid Mech* 28:44–47
6. Qiu GQ, Riffat SB (2010) Experimental investigation on a novel air dehumidifier using liquid desiccant. *Int J Green Energy* 7:174–180

7. Liu XH, Jiang Y, Qu KY (2007) Heat and mass transfer model of cross flow liquid desiccant air dehumidifier/regenerator. *Energy Convers Manage* 48:546–554
8. Oberg V, Goswami DY (1998) Experimental study of the heat and mass transfer in a packed bed liquid desiccant air dehumidifier. *J Sol Energy Eng* 120:289–297
9. Luo Y, Shao S, Xu H, Tian C, Yang H (2014) Experimental and theoretical research of a fin-tube type internally-cooled liquid desiccant dehumidifier. *Appl Energy* 133:127–134
10. Zhang LZ, Niu JL (2003) A pre-cooling Munters environmental control desiccant cooling cycle in combination with chilled-ceiling panels. *Energy* 28:275–292
11. Patanwar P, Shukla SK (2014) Mathematical modelling and experimental investigation of the hybrid desiccant cooling system. *Int J Sustain Energy* 33:103–111
12. Tu M, Ren CQ, Zhao ZS (2010) Performance comparison between two novel configurations of liquid desiccant air conditioning system. *Build Environ* 45:2808–2816
13. Zhao K, Liu XH, Zhang T, Jiang Y (2011) Performance of temperature and humidity independent control air conditioning system applied in an office building. *Energy Build* 43:1895–1903
14. Zhang T, Liu X, Jiang J, Chang X, Jiang Y (2013) Experimental analysis of an internally-cooled liquid desiccant dehumidifier. *Build Environ* 63:1–10
15. Saman WY, Alizadeh S (2002) An experimental study on a cross flow type plate heat exchanger for dehumidification/cooling. *Sol Energy* 73:59–71
16. Yin Y, Zhang X, Wang G, Luo L (2008) Experimental study on a new internally cooled/heated dehumidifier/regenerator of a liquid desiccant systems. *Int J Refrig* 31:857–866
17. Liu XH, Chang XM, Xia JJ, Jiang Y (2009) Performance analysis on the internally cooled dehumidifier using liquid desiccant. *Build Environ* 44:299–308
18. Yin Y, Zhang X, Peng D, Li X (2009) Model validation and case study on internally cooled/heated dehumidifier/regenerator of liquid desiccant systems. *Int J Therm Sci* 48:1664–1671
19. Luo Y, Shao S, Xu H, Tian C, Yang H (2014) Experimental and theoretical research of a fin-tube type internally cooled liquid desiccant dehumidifier. *Appl Energy* 139:127–134
20. Liu J, Zhang T, Liu X, Jiang J (2015) Experimental analysis of an internally-cooled/heated liquid desiccant dehumidifier/regenerator made of thermally conductive plastic. *Energy Build* 99:75–86
21. Kessling W, Laevemann E, Kapfhammer C (1998) Energy storage for desiccant cooling systems component development. *Sol Energy* 64:209–221
22. Queiroz AG, Orlando AF, Saboya FEM (1998) Performance analysis of an air drier for a liquid dehumidifier solar air conditioning system. *J Sol Energy Eng* 110:120–124
23. Bansal P, Jain S, Moon C (2011) Performance comparison of an adiabatic and an internally cooled structured packed-bed dehumidifier. *Appl Therm Eng* 31:14–19
24. Khan AY (1998) Cooling and dehumidification performance analysis of internally-cooled liquid desiccant absorbers. *Appl Therm Eng* 18:265–281
25. Chang XM, Liu XH, Jiang Y (2007) Performance numerical analysis on an internally cooled liquid desiccant dehumidifier. In: *Proceeding IBPSA International Building Performance Simulation Association Conference*, pp 607–613
26. Gao WZ, Shi YR, Cheng YP, Sun WZ (2013) Experimental study on partially cooled dehumidification in liquid desiccant air condition system. *Energy Build* 61:202–209
27. Koronaki IP, Christodoulaki RI, Papaefthimiou VD, Rogdakis ED (2013) Thermodynamic analysis of a counter flow adiabatic dehumidifier with different liquid desiccant materials. *Appl Therm Eng* 50:361–373